Fast Adaptation with Linearized Neural Networks

Wesley J. Maddox[*]
New York University
wjm363@nyu.edu

Shuai Tang[*]
UC San Diego
shuaitang93@ucsd.edu

Pablo Garcia Moreno
Amazon, Cambridge
morepabl@amazon.com

Andrew Gordon Wilson
New York University
andrewgw@cims.nyu.edu

Andreas Damianou
Amazon, Cambridge
damianou@amazon.com

[*]Work partly completed during internship at Amazon.

Abstract

The inductive biases of trained neural networks are difficult to understand and, consequently, to adapt to new settings. We study the inductive biases of linearizations of neural networks, which we show to be surprisingly good summaries of the full network functions. Inspired by this finding, we propose a technique for embedding these inductive biases into Gaussian processes through a kernel designed from the Jacobian of the network. In this setting, domain adaptation takes the form of interpretable posterior inference, with accompanying uncertainty estimation. This inference is analytic and free of local optima issues found in standard techniques such as fine-tuning neural network weights to a new task. We develop significant computational speed-ups based on matrix multiplies, including a novel implementation for scalable Fisher vector products. Our experiments on both image classification and regression demonstrate the promise and convenience of this framework for transfer learning, compared to neural network fine-tuning. Code is available at `https://github.com/amzn/xfer/tree/master/finite_ntk`.

Proceedings of the 24[th] International Conference on Artificial Intelligence and Statistics (AISTATS) 2021, San Diego, California, USA. PMLR: Volume 130.

1 INTRODUCTION

Deep neural networks (DNNs) trained on a source task can be used for predicting in a new (target) task through a process which we interchangeably refer to as transfer learning or domain adaptation (Montavon et al., 2012; Bengio, 2012; Yosinski et al., 2014; Sharif Razavian et al., 2014). One family of approaches to solve this problem adapts the parameters of the full source task network, through gradient descent or more elaborate methods such as meta-learning (Finn et al., 2017). However, adaptation of the network is computationally demanding and prone to getting trapped in local minima. Moreover, fine-tuning the full network in excess can lose a useful representation that was learned from the source domain.

A compelling alternative is to fine-tune only the last layer of the source network, which leads to a log-convex problem that avoids local optima issues and, at the same time, provides a more computationally affordable and less data demanding solution. However, the resulting solution can lead to a poor fit when dealing with complex transfer learning tasks due to the lack of flexibility. Moreover, it is not clear how many of the last layers one would need to fine-tune and what are the overall inductive biases that are transferred to the target task in each case after these layers' parameters have been moved from their original states.

In this paper we aim to address the limitations of fine-tuning with minimal computational overhead, while keeping the performance competitive with costly and involved solutions based on adapting the full network. We propose to structure the transfer learning problem in the following simpler way: firstly, we linearize the DNN with a first order Taylor expansion, giving rise to a linear model whose inductive biases we study here

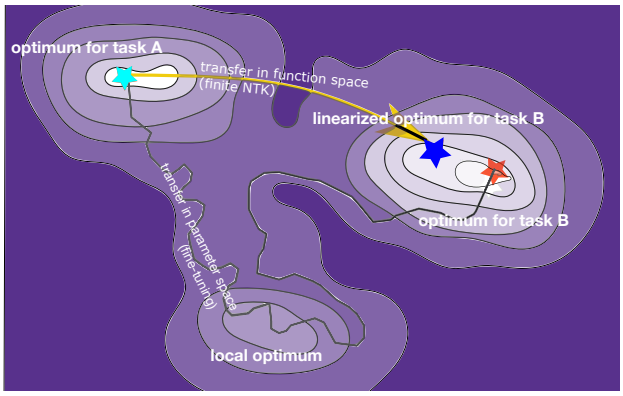

Figure 1: Schematic of our approach to probabilistic transfer learning. We show the loss surfaces for the model as we transfer from the source task (light blue star) to the target task (red/blue stars). Linearizing the network allows for transferring in *function* space which gives a direct mapping to an optimum, while transferring in parameter space (e.g. fine-tuning) can get stuck in local optima.

empirically. Secondly, we embed these inductive biases into a probabilistic lightweight framework which takes the form of a Bayesian linear model with the DNN Jacobian matrix $\boldsymbol{J}$ as the features or, equivalently, a Gaussian process (GP) with $\boldsymbol{J}^\top \boldsymbol{J}$ as the kernel. The kernel matrix is the finite width counterpart of the neural tangent kernel (NTK) (Jacot et al., 2018; Lee et al., 2019) but, crucially, our Taylor expansion is performed around a *trained* model, rather than a randomly initialized one. We then achieve fast adaptation by computing the Jacobian matrix on the target task and invoking the GP predictive equations.

We therefore cast domain adaptation as posterior inference in function space. This solution is analytic (and closed-form, for regression), hence by-passing local optima issues. It is also interpretable: firstly, all of our prior assumptions are encoded in the kernel of the GP, whose inductive biases we study; secondly, our probabilistic model gives a calibrated estimate of the uncertainty of the transfer task and closed form predictive distributions for regression. Figure 1 sums up our approach to transfer learning. Given a trained model at a global optimum (purple star), we transfer in function space using the linearized model to another optimum (red star) avoiding local optima issues incurred by transferring in parameter space using fine-tuning.

To make our approach competitive with respect to non-probabilistic domain adaptation methods we need to tackle one remaining challenge: scalable inference. To this end, we consider a black box inference framework which uses implicit Jacobian vector products and, hence, avoids forming the kernel explicitly. This is complemented by a novel implementation of a directional derivative based on Fisher vector products to enable fast black-box conjugate gradients optimization and test-time caching for fast predictive variances (Gardner et al., 2018; Pleiss et al., 2018). Overall, we are thus able to combine the benefits of probabilistic and neural network models without sacrificing scalability.

Historically, linearizing a sophisticated non-linear trained model dates back at least several decades in machine learning, including Laplace approximations (MacKay, 1992), and perhaps most notably the Fisher kernel (Jaakkola and Haussler, 1998), and related approaches involving Gaussian processes (Seeger, 2002). Interest has recently reignited in these approaches. Beyond the original version of this paper (Maddox et al., 2019), Khan et al. (2019) also used linearized networks, but for tuning hyper-parameters of neural network architectures. Specifically, they used weight parameters derived from variational interpretations of stochastic gradient descent. In other work, Mu et al. (2020) use some of the gradients of unsupervised deep models to transfer to labelled data. Both approaches share some aspects of our construction, using the neural tangent kernel at finite width with trained networks, rather than networks at initialization (Jacot et al., 2018).

We consider applications in both regression and classification. Our key contributions are as follows:

- We study empirically the inductive biases of the linearized DNN model, demonstrating that the linearized model still maintains the strong capabilities of the full neural network for transfer learning.
- We include neural networks in a probabilistic framework by considering the aforementioned linearized DNN model. We develop techniques for fast inference, including a novel implementation for scalable Fisher vector products.
- We apply this probabilistic framework to domain adaptation, casting transfer learning as posterior inference in function space. We demonstrate that this produces strong performance compared to fine-tuning.

The rest of the paper is organized as follows: in Section 2 we summarize related work using the Jacobian matrix of neural networks, in Section 3 we describe how we efficiently use the Jacobian matrix in either a Bayesian (generalized) linear model or a degenerate Gaussian process. In Section 4, we test the inductive biases of these Jacobian kernels. Finally, in Section 5, we test their domain adaptation abilities, demonstrating that they are a strong principled baseline for fast adaptation.

2 RELATED WORK

Using the gradients of a model (such as a DNN) as features for classification problems has a long history. The Fisher kernel used both the Jacobian and inverse Fisher matrices of a generative unsupervised model as the kernel for support vector machines (SVMs) Jaakkola and Haussler (1998). More recently, Zhai et al. (2019) constructed Fisher vectors from GANs and used them to produce highly accurate linear models on CIFAR10. Zinkevich et al. (2017) demonstrated that linear models can be constructed from the Jacobians of DNNs to match the predictions of the full DNN on the training set. Tosi et al. (2014) and Tosi (2014) interpreted the Jacobian matrices for different tasks as creating a probabilistic metric tensor whose expectation is the average Fisher information across several tasks. Finally, we note that model linearization using the Jacobian can be linked to Laplace approximation (MacKay, 2003).

Empirical evidence has shown that features across neural networks are transferable (Bengio, 2012). In particular, Yosinski et al. (2014) and Li et al. (2015) found that features learned by neural networks were transferable across both tasks and architectures. These empirical results motivate our work as the Jacobian is a transformation of the features of the network. More recently, (diagonal) Fisher matrices for classifiers have been shown to be informative for estimating similarity across tasks (Achille et al., 2019). This paper is a longer version of our original work (Maddox et al., 2019), which linearizes trained neural networks for transfer learning. Mu et al. (2020) also consider transfer learning, arguing that the Jacobian is useful for representation learning because it is a local linearization of fine-tuning. They use the Jacobian of several layers of the neural network, rather than the whole network, to transfer deep unsupervised models to become supervised ones. We compare to their approach in Section 5.

Jacot et al. (2018) showed that infinitely wide DNNs behaved as their associated Taylor expansion around *initialization*, terming the resultng kernel in the infinite limit the neural tangent kernel (NTK). Lee et al. (2019) extended their analysis showing that the evolution of finitely wide DNNs over the course of training is similar to that of linear models. Lee et al. (2019) and Arora et al. (2019) gave implementations of infinitely wide DNNs, demonstrating strong performance on CIFAR-10. Due to the analytic nature of these computations, the DNNs studied are restricted: allowing no batch normalization and a slim choice of layers, and use a different scaling than standard DNNs.

Khan et al. (2019) use Jacobian features and a variational distribution in weight space derived from a linear model to tune neural network hyperparameters. They also exploit the GP kernel trick to turn their linear model into a GP, but due to computational concerns only use the diagonal of the Jacobian. After the initial publication of our work, Pan et al. (2021) proposed a similar function space approach but for continual learning that uses the Jacobian matrix and a Laplace approximation. Similarly, Immer et al. (2021) have recently proposed an approach to exploit generalized linear models and the linearization to improve predictions.

3 LINEARIZED NEURAL NETWORK MODEL

We first relate using the Jacobian matrix as features to degenerate Gaussian processes. Given an arbitrary neural network, f, with p parameters θ and n inputs $x = \{x_i\}_{i=1}^n$ with outputs in dimension o, we may Taylor expand f around θ in the following manner:

$$f(x;\theta') \approx f(x;\theta) + \boldsymbol{J}_\theta(x)^\top(\theta - \theta'), \tag{1}$$

where $\boldsymbol{J}_\theta(x)$ is the $p \times on$ Jacobian matrix of the model.[1] We will term Eq. 1 the *linearized NN* model and will consider additionally the first-order approximation as their own model, $g(x;\theta') \approx \boldsymbol{J}_\theta(x)^\top(\theta - \theta')$. Interestingly, this model can be seen as a version of the neural tangent kernel (Jacot et al., 2018) but at finite width, so we refer to it as the finite NTK. For regression, the two models (finite NTK and linearized NN) only differ in the choice of the mean function, which is somewhat unimportant in comparison to the covariance, so we will focus our experiments on the finite NTK.

As our primary goal is to account for functional uncertainty in new tasks, we will consider the linearized model in a Bayesian setting, assigning a prior to the linearized parameters, θ'. We assume that $\theta' \sim \mathcal{N}(0, \boldsymbol{I}_p)$ for simplicity as in Jacot et al. (2018); however, more highly structured Gaussian priors could be used. Under the Gaussian prior assumption, the linearized model and the gradient model are degenerate Gaussian processes (so named because in function space, the resulting kernel is degenerate — i.e. it has a finite number of features) (Rasmussen and Williams, 2008). Both models have the same kernel, $k(x_i, x_j) = \boldsymbol{J}_\theta(x_i)^\top \boldsymbol{J}_\theta(x_j)$, but different mean functions. In contrast to Jacot et al., we take the Taylor expansion around a trained neural network rather than the network at initialization.

[1] We will drop the dependency on x and squeeze o outputs.

3.1 Function Space Updates for Regression

Following Rasmussen and Williams (2008), the predictive posterior over the function f^* on new inputs x^* is:

$$f^*|x^*, \mathcal{D} \sim \mathcal{N}\left(\boldsymbol{J}_\theta^{*\top}(\boldsymbol{J}_\theta\boldsymbol{J}_\theta^\top + \sigma^2\boldsymbol{I}_p)^{-1}\boldsymbol{J}_\theta\boldsymbol{y}, \sigma^2\boldsymbol{J}_\theta^{*\top}(\boldsymbol{J}_\theta\boldsymbol{J}_\theta^\top + \sigma^2\boldsymbol{I}_p)^{-1}\boldsymbol{J}_\theta^*\right) \quad (2)$$

where $\boldsymbol{J}_\theta^*$ is the Jacobian matrix on the new data points.[2] We can now clearly see that inference (and predictive variance computation) only involves inverting a $p \times p$ matrix, e.g. *solving the linear system* $(\boldsymbol{J}_\theta\boldsymbol{J}_\theta^\top + \sigma^2\boldsymbol{I}_p)x = b$, with the Gram matrix, $\boldsymbol{J}_\theta\boldsymbol{J}_\theta^\top$. Naively, this operation requires $\mathcal{O}(p^3)$ time as the linear system is solved in parameter space (the weight space view). Fortunately, we can flip the computations in the dual function space by interpreting $\boldsymbol{J}_\theta$ as producing a degenerate Gaussian process with kernel matrix $\boldsymbol{J}_\theta^\top\boldsymbol{J}_\theta$. Using Woodbury's matrix identity, the posterior predictive distribution can be re-written as:

$$f^*|x^*, \mathcal{D} \sim \mathcal{N}\left(\boldsymbol{J}_\theta^{*T}\boldsymbol{J}_\theta(\boldsymbol{J}_\theta^\top\boldsymbol{J}_\theta + \sigma^2\boldsymbol{I}_n)^{-1}\boldsymbol{y}, \sigma^2\boldsymbol{J}_\theta^{*T}(\boldsymbol{I}_p - \boldsymbol{J}_\theta(\boldsymbol{J}_\theta^\top\boldsymbol{J}_\theta + \sigma^2\boldsymbol{I}_n)^{-1}\boldsymbol{J}_\theta^\top)\boldsymbol{J}_\theta^*\right) \quad (3)$$

Again, inference only requires solving the linear system $(\boldsymbol{J}_\theta^\top\boldsymbol{J}_\theta + \sigma^2\boldsymbol{I}_n)x = b$, naively requiring $\mathcal{O}(n^3)$ time as the linear system is solved in function space (the function space view). Popular neural networks are generally over-parameterized, containing many more parameters than training samples; therefore, the function-space view will typically be faster. In the following section, we will consider computational considerations.

Extension to Non Gaussian Likelihoods: For non-Gaussian likelihoods, a degenerate Gaussian process on the latent functions is again produced, equivalent now to a Bayesian generalized linear model (GLM). Specifically, for multi-class classification the GLM contains the Jacobian within a categorical likelihood:

$$p_{\text{lin}}(y_i|x,\theta) = \text{Cat.}\left(y_i|\frac{\exp\{\boldsymbol{J}_\theta^\top\theta'\}}{\sum_{i=1}^C \exp\{\boldsymbol{J}_\theta^\top\theta'\}}\right), \quad (4)$$

with appropriate reshaping to account for the *on* outputs of the model. Unfortunately, the posterior over θ' cannot be computed in closed-form. We consider both Laplace approximations and stochastic variational inference (Hoffman et al., 2013). See Appendix A for details.

3.2 Computational Speed-Ups

To consider large DNNs within our approach, we need to tackle two scalability issues: firstly the Jacobian matrix is not closed form for most NN models, and secondly, GP inference scales poorly. We resolve both issues simultaneously by using implicit Jacobian vector and vector Jacobian products as implemented in standard automatic differentiation software like Pytorch (Paszke et al., 2019). Implicit Jacobian vector products never form the full Jacobian matrix and use three backwards calls, one to compute $\boldsymbol{J}_\theta^\top v$ and two for $\boldsymbol{J}_\theta v$, rather than n. They are also extremely compatible with conjugate gradient (CG) approaches for GP inference (e.g. GPyTorch), as CG only requires matrix vector multiplications, resolving the poor scaling of GP inference. CG-enabled GP inference reduces the inference complexity from $\mathcal{O}(n^3)$ to $\mathcal{O}(n^2)$, while keeping the memory required constant by not forming dense matrices unnecessarily (Gardner et al., 2018). More implementation details are in Appendix B.

To demonstrate the efficiency of combining CG-enabled GP inference with implicit Jacobian vector products, we performed experiments with up to $100,000$ data points using five layer perceptrons with about $800,000$ parameters using only a single GPU. We show the timing in Figure 2, finding that predictive means and variances can be computed in under five minutes on even the largest models and datasets. We used similar architectures in Section 5.

For further computational improvements, we can perform inference in parameter space by leveraging the Jacobian's relationship to the Fisher information matrix, which is defined as. $\mathbb{F}(\theta) := \mathbb{E}_{p(x,y|\theta)}(\nabla_\theta \log p(y|x,\theta)\nabla_\theta \log p(y|x,\theta)^\top)$. For Gaussian likelihoods, the Fisher information matrix is proportional to the outer product of the Jacobian matrix with itself, e.g. $\boldsymbol{J}\boldsymbol{J}^\top \propto \mathbb{F}(\theta)$, across a dataset.

To exploit the relationhip, we derived a novel finite differences Fisher vector product (FVP) via the derivative of the Kullback-Leiber (KL) that gives matrix vector products with only one backwards call. The second order Taylor expansion of the KL divergence between two distributions, $p(y|\theta)$ and $p(y|\theta')$, with parameters θ and θ' is given by:

$$D_{\text{KL}}(p(y \mid \theta)||p(y \mid \theta')) = \frac{1}{2}(\theta - \theta')^\top\mathbb{F}(\theta)(\theta - \theta') + \mathcal{O}(\theta - \theta')^3.$$

Evaluating the derivative at $\theta' = \theta + \epsilon v$ gives:

$$\nabla_\theta D_{\text{KL}}(p(y \mid \theta)||p(y \mid \theta'))|_{\theta'=\theta+\epsilon v} = \epsilon\mathbb{F}(\theta)v + \mathcal{O}(\epsilon^2||v||). \quad (5)$$

Therefore, to compute Fisher vector products, we merely need to compute a second forwards pass with θ', compute the KL divergence in likelihood space between the model with parameters θ and the model with

[2] Dropping the dependency on x^* for a superscript and using $\boldsymbol{y}$ to include both the response and the mean terms $\mu_\theta(x) = \boldsymbol{J}_\theta^\top\theta + f_\theta(x)$.

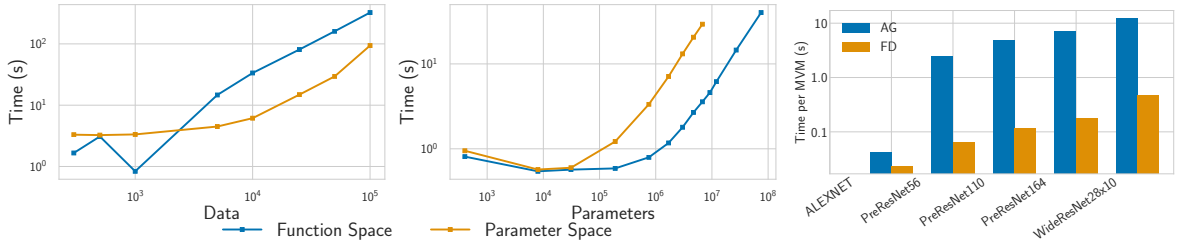

Figure 2: **Left:** Nearly linear scaling time of log probability calculation for an $\approx 800,000$ parameter MLP as a function of n. **Center:** Nearly linear scaling time of log probability calculation for $1,000$ data points as a function of model size. In both situations, both the function-space approach and the parameter space approach scale particularly well, reaching $100,000$ data points (and nearly 100 million parameters) unlike standard GP training procedures which are $\mathcal{O}(n^3)$. **Right:** Speedup of finite differences (FD) Fisher-vector products against autograd (AG) for AlexNet (Krizhevsky et al., 2012), PreResNets (He et al., 2016) of varying depth, and WideResNet (Huang et al., 2017) on CIFAR-10. Our method typically achieves a 30× speedup over the standard implementation, demonstrating the practical utility of our approach to working with the Fisher matrix.

parameters θ', and then backpropagate with respect to θ'. The resulting gradient, up to error, is proportional to $\mathbb{F}(\theta)v$. To use these FVPs to increase the speed of our GP implementation, we use CG to solve systems of equations in parameter space (e.g. Eq. 2) replacing matrix vector multiplications of the form $\boldsymbol{J}_\theta \boldsymbol{J}_\theta^\top v$ with $a\mathbb{F}(\theta)v$, where a is the appropriate scaling constant. In Figure 2, we show the efficiency of finite NTK inference using these finite differences (FD) FVPs in comparison to kernel space inference. We also show the speedup against an exact FVP computed using autograd (AG), where the FD version is about 30× faster across a variety of modern architectures. Accuracy is not affected as relative error typically is on the order of 0.001. Exact implementation details are in Appendix C.

3.3 Fast Adaptation Modelling

There is a long history of multi-task Gaussian process models, see Álvarez et al. (2012) for further discussion. We adopt the simplest multi-task model, which considers the parameters of the trained neural network to be shared across all tasks, and recomputing the Jacobian for each new task (equivalent to sharing the kernel hyper-parameters across tasks).

The generative process can be described as follows: first, the dataset is drawn from a dataset distribution $\mathcal{D}_t = (x_t, y_t) \sim p(\mathcal{D})$, so that, for each individual task and dataset, $\mathcal{D}_t$, we have the likelihood $p(\boldsymbol{y}_t|x_t) = p(\boldsymbol{y}_t|f_{\theta_t}(x_t))$. In our setting, we have the linearized neural network, $f_t \approx \boldsymbol{J}_\theta(x_t)\theta_t' + \mu(x_t)$, where $\boldsymbol{J}_\theta(x) = (\nabla_\theta f(x))^\top \in \mathbb{R}^{p\times on}$, and $\mu(x,t)$ is the GP mean function as described previously, and θ_t' are the parameters of the (Bayesian) linearized model. The kernel for each task is given by $\boldsymbol{J}_\theta(x_t)^\top \boldsymbol{J}_\theta(x_t')$ as in Section 3.1. Note that the Jacobian computation depends only on the parameters θ of the pre-trained network. We can then represent the functions f_t (for other tasks) in a way that does not involve a new non-convex optimization. Thus, our procedure only requires a pretrained neural network on an initial task. When a new task is presented, the Jacobian matrix of data samples in the given task w.r.t. the pretrained parameters is used to derive the predictive distribution of the GP, which only requires solving a linear system. We present the overall algorihtm in Algorithm 1. In Appendix D we further describe the domain adaptation model.

4 INDUCTIVE BIASES OF LINEARIZED NEURAL NETWORKS

We first investigate the inductive biases of linearized neural networks on both regression and classification on CIFAR10, while showing that the Jacobians of similar tasks are related. Overall, we demonstrate i) that linearized neural networks retain the inductive biases of their nonlinear counterparts and ii) that the Jacobian matrix is a useful inductive bias for transfer learning.

Qualitative Regression Experiments: We begin with demonstrating qualitatively that linearized neural networks retain good inductive biases. See Appendix E for training and dataset details. First, in Figure 3a, we show the fit of the ReLU network trained on a synthetic dataset, alongside the posterior predictive mean and variance of the resulting Gaussian process. We do so for both trained and un-trained networks. Pleasingly, in both cases, having enough hidden units (in this case, 5000) gives reasonable predictions.

Second, in Figure 3b, we show the effect of different architectures on a different synthetic dataset. We can again qualitatively see that architectures that have

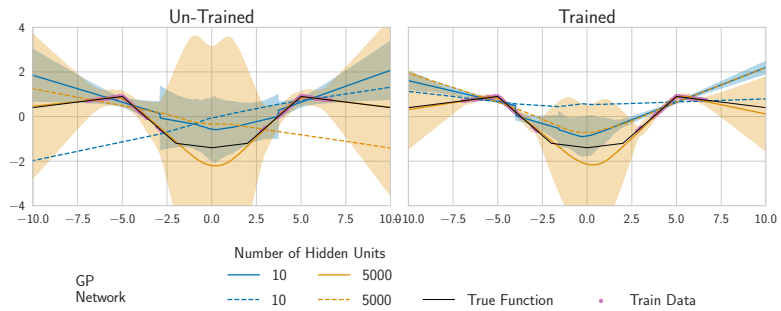

(a) Trained and untrained ReLU networks with one hidden layer.

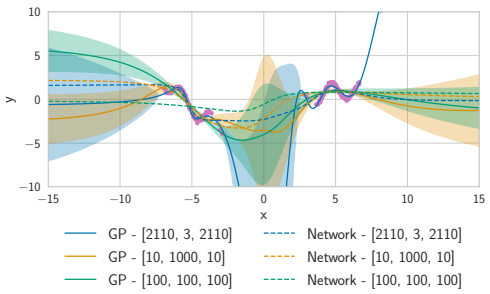

(b) Trained tanh networks of different widths.

Figure 3: Posterior means and confidence regions, $p(f^*|y)$, for MLPs of varying width and depth. Solid lines are the predictive means from the linearized neural network, with shading corresponding posterior confidence region; dashed lines are predictions from the full neural network. The observed data is shown as pink dots. **Left:** Linearization of un-trained single-layer ReLU networks of varying width. **Center:** Linearization for trained networks. Observable in both plots is the increase in the GP predictive variances as a function of width due to using standard initializations, while the trained networks have less predictive variance, especially around the training data (due to being fit on the data). **Right:** Three layer tanh architectures with different widths but similar numbers of parameters trained on a sinusoidal regression problem. Not only are the network's predictions qualitatively different, but their linearizations also are significantly different outside of the training data.

Algorithm 1 Domain Adaptation Procedure

Input: Data $(\boldsymbol{X}_1, \boldsymbol{y}_1)$, Initial parameters θ_0
Compute θ_{MLE} with data $(\boldsymbol{X}_1, \boldsymbol{y}_1)$.
Transfer inductive biases to GP:
$f \sim \mathcal{GP}(0, k = \mathbf{J}(\mathbf{x}_1; \theta_{MLE})^\top \mathbf{J}(\mathbf{x}_1; \theta_{MLE}))$
Compute Jacobian for task t: $\mathbf{J}_t = \mathbf{J}(\mathbf{x}_t; \theta_{MLE})$
Adapt f to domain t using Eq. 3 and $\mathbf{J}_t$:
$p(f_t^*|\mathcal{D}_t) = \int p(f^*|\theta_t')p(\theta_t'|\mathcal{D}_t)d\theta'$

good fits to the data (e.g. not over-fit) tend to also have reasonable predictive means and variances (e.g. the predictive mean fits the training data well and the predictive variance increases away from the data). We choose three separate architectures that all have about $21,000$ parameters, but differing numbers of hidden units at each layer to test the hypothesis that the performance of the linearized NN is tied to the over-parameterization effect rather than the architecture itself. Given that performance vastly differs even in this simple setting, we attribute the performance to the architecture itself, rather than over-parameterization.

Linearized PreResNets on CIFAR-10: We next tested the accuracy, test loglikelihood (NLL), and expected calibration error (ECE) (Guo et al., 2017) for PreResNets of varying depth on CIFAR10, displaying these results in Figure 4. Here, using the Jacobian matrices as features for classification leads to highly competitive performance for Bayesian generalized linear models — about 92% with our VI approximation for the standard 56 layer version. By comparison the top known kernel method (infinite un-trained neural network, but with a different architecture) on CIFAR-10 seems to be the result of Li et al. (2019), which is about 89%. Further results with MAP inference and Laplace approximations are in Appendix F. Intriguingly, we also find that the linearized networks here are more-overconfident (higher ECE) than the full model.

Transferability of Jacobian Features: Thus far, we have demonstrated that the Jacobian matrix is useful merely for a single task — e.g. a linearized model is a good inductive bias for both classification and regression. However, we next demonstrate that for a given architecture, the Jacobian matrix is similar across related tasks. We consider trained networks on three different datasets — two halves of MNIST (MNIST1 and MNIST2) (LeCun et al., 1998), and FMNIST (Xiao et al., 2017). MNIST1 and MNIST2 are similar because they come from the same distribution, so we expect that classifiers trained on MNIST1 and MNIST2 will be similar due to being trained on similar data. By the same token, we expect these classifiers to have different representations than a classifier trained on FMNIST, which is images of clothing.

To test our hypothesis, we trained 25 LeNet-3 (LeCun et al., 1998) networks each on the three datasets, and then computed the full Jacobian matrix of each model on 5000 images from MNIST1[3]. Next, we computed the similarity of the matrices via their squared cosine similarity, e.g. $\text{sim}(A, B) = \frac{tr(A^\top BB^\top A)}{||AA^\top||_F||BB^\top||_F}$. We show

[3]We fine-tuned the final layer of the FMNIST networks to remove distinctions in class labels and predictions.

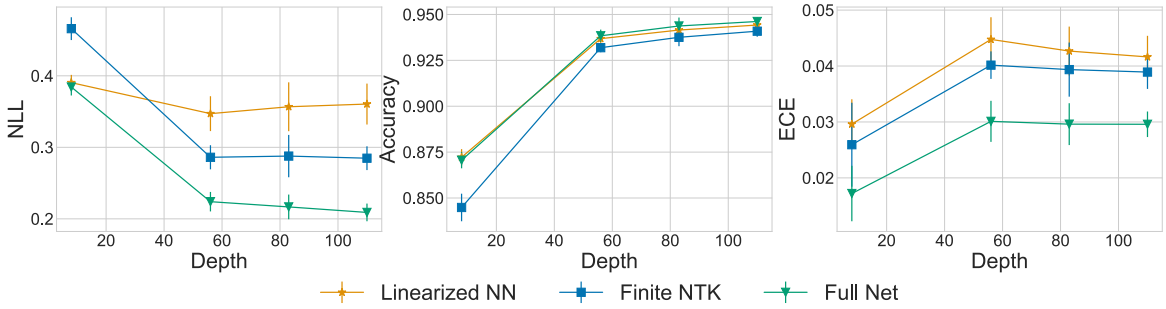

Figure 4: Test negative log-likelihood (NLL), accuracy, and expected calibration error (ECE) of PreResNets varying depth and their linearized counterparts as a function of depth on CIFAR-10, averaged over 10 seeds. For the linearization, we use a VI approach. Both the linearized NN (orange) and the finite NTK (blue) perform well in terms of accuracy, nearly comparable to the full network (green). However, they perform slightly worse relatively in terms of NLL and ECE, implying that they are more over-confident about their predictions.

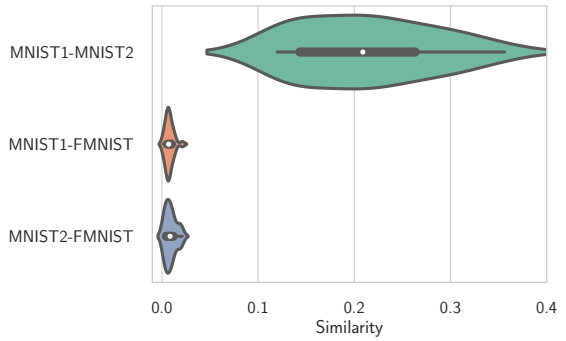

Figure 5: Cosine similarities of the Jacobians of trained LeNet-3s on the first half of MNIST (MNIST1). Models trained on FMNIST and evaluated on MNIST1 are less similar to models trained directly on MNIST1 than those trained on the second half of MNIST (MNIST2). The white dot in the middle is the average similarity across 25 random seeds, with the black lines showing the quartiles. The width of the violin for each comparison corresponds to the density estimate across these seeds, showcasing a population.

histograms of the similarities across the 25 comparisons in Figure 5, finding that the Jacobians are vastly more similar between classifiers trained on MNIST1 and MNIST2 (shown in blue), while the classifiers trained on MNIST1 and MNIST2 have nearly zero similarity to those from FMNIST (shown in orange and green). This result supports our hypothesis, suggesting that the Jacobians of two models should be similar to each other if they were trained on similar enough tasks; full training details and the spectrum of the Jacobians for all of the models is shown in Appendix E.1.

5 TRANSFERABILITY EXPERIMENTS

Finally, we demonstrate that, on a variety of regression and classification tasks, our linearization framework enables transfer of the inductive biases from one task to others and enables good representations of uncertainty. Experimental details are in Appendix E, while further results are in Appendix F.

Sinusoids: In Figure 6, we generate 3 datasets and train a three-layer MLP with tanh activations to completion only on the first dataset (the orange points). We plot the fit from the finite NTK in blue (the mean and the confidence region), showing the validation (context) points in purple. We replicate the generative process of Kim et al. (2018), with various periods for the sinusoids. Here, we compare to a trained adaptive basis linear regression (ABLR) model (Perrone et al., 2018) is shown in grey and to transferred RBF Gaussian processes (yellow). ABLR requires many gradient steps to converge on the adaptation task as it continually re-trains the features of the last layer. Additionally, the linearized model performs comparably to transferred hyper-parameter RBF GPs which are close to the gold standard on this task, because the functions are smooth. However, the linearized model gives reasonable posterior predictive *distributions* like the GP. In Appendix F.3, we additionally compare to transferring the deep kernel learning latent space, and adaptive deep kernel learning (Tossou et al., 2019), finding again that these alternative approaches underfit.

Malaria Prediction: Inspired by Balandat et al. (2020), we used data describing the infection rate of *Plasmodium falciparium* (a malaria causing parasite)

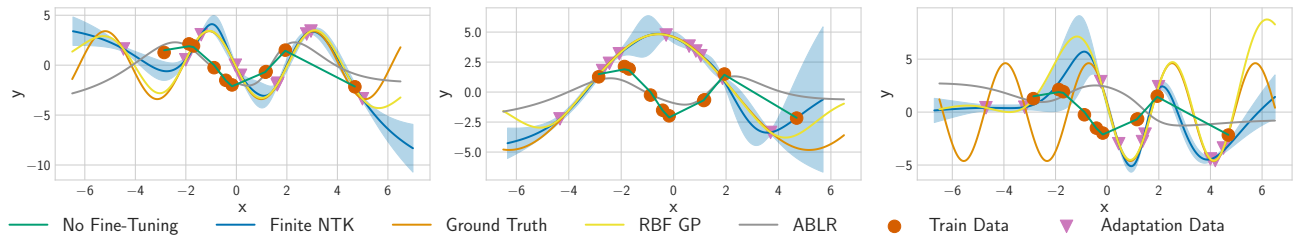

Figure 6: Posterior predictions on a few shot regression task using the finite NTK (blue). We performed training on the orange points, while adapting to the purple points (context), viewing each function as an independent draw from the GP described in Section 3.3. The comparisons here are RBF GPs fit on the source task with the hyper-parameters shared across tasks (yellow) and adaptive Bayesian linear regression (ABLR) (gray) (Perrone et al., 2018). Our finite NTK approach improves upon the RBF kernel, and significantly outperforms ABLR.

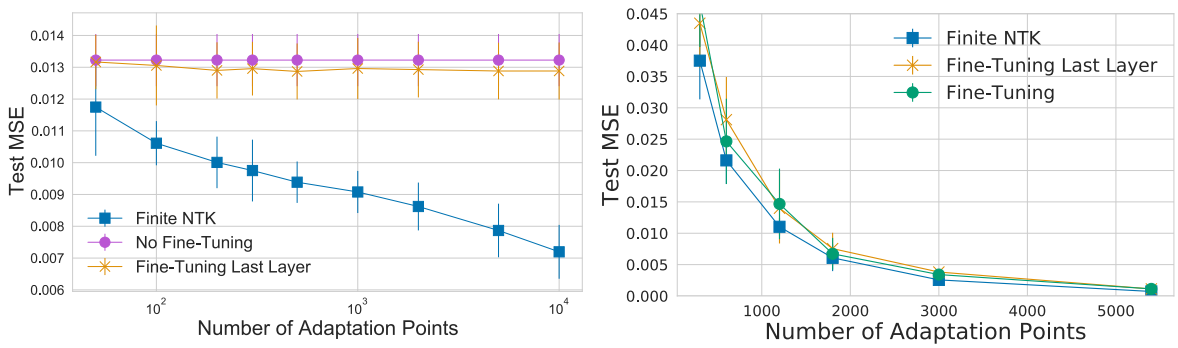

(a) Malaria dataset

(b) Olivetti faces dataset

Figure 7: **(a)** Error on held out set for infection rate of *Plasmodium falciparium* among African children. The NTK improves its accuracy on the held-out set as the number of validation data points from 2016 are given to it, while re-training the last layer stagnates and only has marginally better performance than no-retraining at all. **(b)** Error on held out set on the Olivetti fast adaptation task. In this setting, all methods improve with more adaptation points, and the NTK has the biggest advantage when there is a small amount of data for transfer.

Table 1: Test Accuracy on CIFAR10 for linearizing different layers of the BiGAN encoder. $*$ denotes numbers reproduced from Table 1 of Mu et al. (2020), which are included as baselines. Using all of the layers produces slightly better results than using only the top layers. All linearization settings are best compared to the activation baseline of 62.87% which consists of training a classifier on top of the feature extractor. Fine-tuning all of the layers is also better overall.

Layers	Top Layer	Top 2 Layers	Top 3 Layers	All Layers	All Layers (VI)
Fine-tuning	71.78*	73.18*	74.30*	*77.25*	-
Finite NTK	70.28*	71.08*	70.64*	***72.65***	*71.89*

drawn from the Malaria Global Atlas[4] in a domain adaptation task. We trained a heteroscedastic neural network with three layers on 2000 data points from the 2012 map, before testing on varying numbers of data points from the 2016 map. In Figure 7a, we show the test MSE for no re-training, the Jacobian as the kernel, and retraining the final layer versus the validation points given from the 2016 map. The performance of the Jacobian kernel as a transfer model improves as the number of data points given to it at validation time increases. For a fixed training budget (the same as the original training epochs), the re-trained last layer stagnates in performance. By contrast, re-training the last layer for $6x$ the training epochs will give comparable results to the finite NTK, but at a significantly increased computational expense; see Appendix E for further details.

Image Pose Prediction: We next convert the image rotation prediction task in Wilson et al. (2016) on the publicly available Olivetti Faces dataset.[5] We used a similar version of the LeNet-3 architecture for this task

[4]Extracted from `https://map.ox.ac.uk`.

[5]`scikit-learn.org/0.19/datasets/olivetti_faces.html`.

(LeCun et al., 1998). To construct this task, we used all 40 faces and rotated them such that $\theta \sim U(0, 30)$ where θ is the degree of rotation, cropping them to fit the 45×45 images, selected 20 faces to serve as the training set and the other 20 to serve as the adaptation set; the targets in all cases are the standardized degree of rotation. From the adaptation set, we randomly selected varying numbers of the data to serve as the adaptation points as we wish to have the methods quickly adapt to the new faces; we then evaluated on the MSE on the remainder of the adaptation points. We find, as displayed in Figure 7b, that the linearized NN performs best across the entirety of the number of adaptation points, although the gains are small when many points are considered.

Transferring Unsupervised Models: We finally test the capability of the linearized model to work as a supervised model when the full model is trained on an un-supervised task, following the experiments of Mu et al. (2020), who used BiGANs (Donahue et al., 2016) trained on CIFAR10 and linearized only the top convolutional layers. We replicate their experimental setup, but consider inclusion of all of the features as well, by adding the Jacobian of the base feature extractor network into the model. Like Mu et al. (2020), we used a fixed projection from the output dimensionality of the network down to 10 output dimensions so that we can perform classification with it. The results are shown in Table 1, where we see that in this problem the top layers seem to be at least as useful as the full gradient projections. Here, the all layers column refers to solely MAP trained models for direct comparison with Mu et al. (2020), while all layers (VI) refers to our finite NTK model with variational inference. We hypothesize that the underperformance of the finite NTK is due to using approximate inference.

6 CONCLUSION

We have shown how it is possible to build scalable kernel methods with the inductive biases of neural networks, but with closed-form training and no local optima, through a linearization. We combine these kernels with Gaussian processes for a principled representation of uncertainty. We show how to make inference scalable by developing efficient techniques for Jacobian vector products and conjugate gradients. The techniques we propose are in fact generally applicable, and in the future could be leveraged in a wide range of other settings where one wishes to perform efficient operations with a Jacobian or Fisher matrix. In this paper, we apply these ideas primarily for fast, convenient, and analytic transfer learning with neural networks. Exciting future work could further develop this direction for meta-learning, where one wishes to efficiently capture the transfer of knowledge across several tasks and uncertainty plays an important role.

Acknowledgements

WJM, AGW are supported by an Amazon Research Award, NSF I-DISRE 193471, NIH R01 DA048764-01A1, NSF IIS-1910266, and NSF 1922658 NRT-HDR: FUTURE Foundations, Translation, and Responsibility for Data Science. WJM was additionally supported by an NSF Graduate Research Fellowship under Grant No. DGE-1839302. We would like to thank Jacob Gardner, Alex Wang, Marc Finzi, and Tim Rudner for helpful discussions, Jordan Massiah for help preparing the codebase, and the NYU Writing Center for writing guidance.

References

Achille, A., Lam, M., Tewari, R., Ravichandran, A., Maji, S., Fowlkes, C., Soatto, S., and Perona, P. (2019). Task2Vec: Task Embedding for Meta-Learning. In *ICCV*.

Álvarez, M. A., Rosasco, L., Lawrence, N. D., et al. (2012). Kernels for vector-valued functions: A review. *Foundations and Trends® in Machine Learning*, 4(3):195–266.

Arora, S., Du, S. S., Hu, W., Li, Z., Salakhutdinov, R., and Wang, R. (2019). On exact computation with an infinitely wide neural net. In *Advances in Neural Information Processing Systems*.

Balandat, M., Karrer, B., Jiang, D. R., Daulton, S., Letham, B., Wilson, A. G., and Bakshy, E. (2020). BoTorch: Programmable Bayesian Optimization in PyTorch. In *Advances in Neural Information Processing Systems*.

Bengio, Y. (2012). Deep Learning of Representations for Unsupervised and Transfer Learning. In *Workshop on Unsupervised and Transfer Learning*, volume 27, page 21. PMLR W&CP.

Donahue, J., Krähenbühl, P., and Darrell, T. (2016). Adversarial feature learning. In *International Conference on Learning Representations (ICLR)*.

Finn, C., Abbeel, P., and Levine, S. (2017). Model-Agnostic Meta-Learning for Fast Adaptation of Deep Networks. In *International Conference on Machine Learning*.

Gardner, J. R., Pleiss, G., Bindel, D., Weinberger, K. Q., and Wilson, A. G. (2018). GPyTorch: Blackbox Matrix-Matrix Gaussian Process Inference with GPU Acceleration. In *Advances in Neural Information Processing Systems*.

Golub, G. H. and Pereyra, V. (1973). The Differentiation of Pseudo-Inverses and Nonlinear Least Squares Problems Whose Variables Separate. *SIAM Journal on Numerical Analysis*, 10(2):413–432.

Guo, C., Pleiss, G., Sun, Y., and Weinberger, K. Q. (2017). On Calibration of Modern Neural Networks. In *International Conference on Machine Learning*.

He, K., Zhang, X., Ren, S., and Sun, J. (2016). Deep Residual Learning for Image Recognition. In *CVPR*. arXiv: 1512.03385.

Hoffman, M. D., Blei, D. M., Wang, C., and Paisley, J. (2013). Stochastic variational inference. *The Journal of Machine Learning Research*, 14(1):1303–1347.

Huang, G., Liu, Z., van der Maaten, L., and Weinberger, K. Q. (2017). Densely Connected Convolutional Networks. In *CVPR*.

Immer, A., Korzepa, M., and Bauer, M. (2021). Improving predictions of Bayesian neural nets via local linearization. *arXiv:2008.08400 [cs, stat]*. arXiv: 2008.08400.

Jaakkola, T. and Haussler, D. (1998). Exploiting Generative Models in Discriminative Classifiers. In *Advances in Neural Information Processing Systems*.

Jacot, A., Gabriel, F., and Hongler, C. (2018). Neural tangent kernel: Convergence and generalization in neural networks. In *Advances in neural information processing systems*.

Khan, M. E., Immer, A., Abedi, E., and Korzepa, M. (2019). Approximate Inference Turns Deep Networks into Gaussian Processes. *arXiv preprint arXiv:1906.01930*.

Kim, T., Yoon, J., Dia, O., Kim, S., Bengio, Y., and Ahn, S. (2018). Bayesian Model-Agnostic Meta-Learning. In *Advances in Neural Information Processing Systems*.

Krizhevsky, A. (2009). Learning Multiple Layers of Features from Tiny Images. page 60.

Krizhevsky, A., Sutskever, I., and Hinton, G. E. (2012). Imagenet classification with deep convolutional neural networks. In *Advances in neural information processing systems*.

LeCun, Y., Bottou, L., Bengio, Y., Haffner, P., and others (1998). Gradient-based learning applied to document recognition. *Proceedings of the IEEE*, 86(11):2278–2324.

Lee, J., Xiao, L., Schoenholz, S. S., Bahri, Y., Novak, R., Sohl-Dickstein, J., and Pennington, J. (2019). Wide Neural Networks of Any Depth Evolve as Linear Models Under Gradient Descent. In *Advances in Neural Information Processing Systems*.

Li, Y., Yosinski, J., Clune, J., Lipson, H., and Hopcroft, J. (2015). Convergent Learning Do different neural networks learn the same representations? In *The 1st International Workshop on Feature Extraction: Modern Questions and Challenges*, volume 44, page 17. PMLR W&CP.

Li, Z., Wang, R., Yu, D., Du, S. S., Hu, W., Salakhutdinov, R., and Arora, S. (2019). Enhanced Convolutional Neural Tangent Kernels. *arXiv:1911.00809 [cs, stat]*. arXiv: 1911.00809.

MacKay, D. J. C. (1992). Bayesian Interpolation. *Neural Computation*.

MacKay, D. J. C. (2003). *Information theory, inference, and learning algorithms*. Cambridge University Press, Cambridge, UK ; New York.

Maddox, W. J., Tang, S., Moreno, P. G., Wilson, A. G., and Damianou, A. (2019). On Linearizing Neural Networks for Transfer Learning. *NeurIPS MetaLearn Workshop*.

Montavon, G., Orr, G. B., and Müller, K., editors (2012). *Neural Networks: Tricks of the Trade - Second Edition*, volume 7700 of *Lecture Notes in Computer Science*. Springer.

Mu, F., Liang, Y., and Li, Y. (2020). Gradients as Features for Deep Representation Learning. In *International Conference on Learning Representations*.

Netzer, Y., Wang, T., Coates, A., Bissacco, A., Wu, B., and Ng, A. Y. (2011). Reading Digits in Natural Images with Unsupervised Feature Learning. In *NIPS Workshop on Deep Learning and Unsupervised Feature Learning*.

Pan, P., Swaroop, S., Immer, A., Eschenhagen, R., Turner, R. E., and Khan, M. E. (2021). Continual Deep Learning by Functional Regularisation of Memorable Past. *arXiv:2004.14070 [cs, stat]*. arXiv: 2004.14070.

Paszke, A., Gross, S., Massa, F., Lerer, A., Bradbury, J., Chanan, G., Killeen, T., Lin, Z., Gimelshein, N., Antiga, L., et al. (2019). Pytorch: An imperative style, high-performance deep learning library. In *Advances in neural information processing systems*, pages 8026–8037.

Patacchiola, M., Turner, J., Crowley, E. J., O'Boyle, M., and Storkey, A. (2019). Deep kernel transfer in gaussian processes for few-shot learning. In *Advances in Neural Information Processing Systems*.

Perrone, V., Jenatton, R., Seeger, M. W., and Archambeau, C. (2018). Scalable Hyperparameter Transfer Learning. In *Advances in Neural Information Processing Systems*, page 11.

Pleiss, G., Gardner, J. R., Weinberger, K. Q., and Wilson, A. G. (2018). Constant-Time Predictive

Distributions for Gaussian Processes. In *Artificial Intelligence and Statistics*.

Rasmussen, C. E. and Williams, C. K. I. (2008). *Gaussian processes for machine learning*. Adaptive computation and machine learning. MIT Press, Cambridge, Mass., 3. print edition.

Saad, Y. (2003). *Iterative methods for sparse linear systems*. SIAM, Philadelphia, Pa, 2. ed edition.

Seeger, M. (2002). Covariance kernels from bayesian generative models. *Advances in neural information processing systems*, 2:905–912.

Sharif Razavian, A., Azizpour, H., Sullivan, J., and Carlsson, S. (2014). CNN Features Off-the-Shelf: An Astounding Baseline for Recognition. pages 806–813.

Tosi, A. (2014). *Visualization and Interpretability in Probabilistic Dimensionality Reduction Models*. PhD Thesis, Universitat Politecnica de Catalunya.

Tosi, A., Hauberg, S., Vellido, A., and Lawrence, N. D. (2014). Metrics for Probabilistic Geometries. In *Uncertainty in Artificial Intelligence*.

Tossou, P., Dura, B., Laviolette, F., Marchand, M., and Lacoste, A. (2019). Adaptive deep kernel learning.

Wilson, A. G., Hu, Z., Salakhutdinov, R., and Xing, E. P. (2016). Deep Kernel Learning. In *Artificial Intelligence and Statistics*. arXiv: 1511.02222.

Xiao, H., Rasul, K., and Vollgraf, R. (2017). Fashion-mnist: a novel image dataset for benchmarking machine learning algorithms. *arXiv preprint arXiv:1708.07747*.

Yang, G. (2019). Scaling limits of wide neural networks with weight sharing: Gaussian process behavior, gradient independence, and neural tangent kernel derivation. *arXiv preprint arXiv:1902.04760*.

Yosinski, J., Clune, J., Bengio, Y., and Lipson, H. (2014). How transferable are features in deep neural networks? In *Advances in Neural Information Processing Systems*.

Zhai, S., Talbott, W., Guestrin, C., and Susskind, J. M. (2019). Adversarial Fisher Vectors for Unsupervised Representation Learning. In *Advances in Neural Information Processing Systems*.

Zinkevich, M. A., Davies, A., and Schuurmans, D. (2017). Holographic feature representations of deep networks. In *Uncertainty in Artificial Intelligence*.